

# $K_3CeP_2S_8$ : A New Cerium Thiophosphate with One-Dimensional Anionic Chains

Gilles Gauthier, Stéphane Jobic,\* Raymond Brec, and Jean Rouxel

Institut des Matériaux de Nantes, Laboratoire de Chimie des Solides, BP 32229, 44322 Nantes Cedex 3, France

Received January 27, 1998

As first demonstrated a decade ago, the  $K_2S/S$  low-melting flux reacts readily with titanium metal, allowing the preparation of  $K_4Ti_3S_{14}$ .<sup>1</sup> This powerful synthetic method, first applied to Ti and then extended to other transition elements, has been successfully widened to main group and rare earth elements, giving rise to a rich structural chemistry.<sup>2–6</sup> Since then, its field of applications has been further enlarged through the substitution of the alkali metal flux by an alkaline earth metal one, reinforcing the ability of this method to explore new domains.<sup>7,8</sup>

From a conceptual point of view, one of the great interests of this reactive flux technique lies in its capacity to control the dimensionality of the covalent network by modifying the nature of the alkali metal and its concentration, to obtain a more or less covalent framework.<sup>9,10</sup> Hence, it is possible to synthesize low-dimensional compounds with their inherent anisotropic chemical and physical properties. An interesting property of these low-dimensional phases is their ability to exfoliate to lead to sols and/or gels. We recently showed that a chain containing  $KNiPS_4$ <sup>11</sup> dissolves in polar organic solvents, leading to autofragmentation of the chains into an unprecedented concave trimetallic trivalent anion.<sup>12,13</sup> In order to have more materials with a 2-, 1-, or even 0D character with potential exfoliation properties, we attempted to stabilize new thiophosphates of cerium and alkali metal through the exploration of the  $A/Ce/P/Q$  system ( $A = Na, K$ ;  $Q = S, Se$ ). In this Communication, we report the synthesis of and band structure calculations on  $K_3CeP_2S_8$ , a new member of the  $(AS)_n-(ACeP_2S_6)_n$  series ( $n = 0, 1, 2$ ;  $A =$  alkali metal).

$K_3CeP_2S_8$  is one of the several members of the  $K-Ce-P-S(Se)$  family among which are found  $KCeP_2S_6$  and  $K_2CeP_2S_7$ ,<sup>14</sup> the structures and properties of which will be published elsewhere.<sup>15</sup> The structure of  $K_3CeP_2S_8$ ,<sup>16</sup> determined from a single-crystal X-ray data analysis,<sup>17,18</sup> is characterized by the occurrence of infinite  $^{1-}[\text{CeP}_2\text{S}_8]^{3-}$  chains electrostatically shielded by surrounding  $K^+$  cations (Figure 1). These chains are built upon

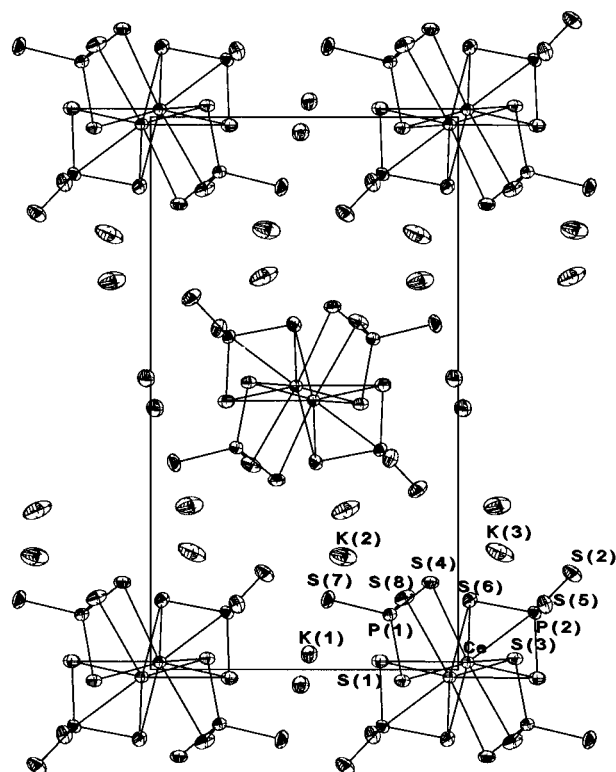


**Figure 1.** View of the structure of  $K_3CeP_2S_8$  (50% probability ellipsoids shown) along the  $a$  axis showing  $^{1-}[\text{CeP}_2\text{S}_8]^{3-}$  chains separated by alkali metals.  $K-S$  bonds have been omitted for clarity.

9-fold sulfur coordinated Ce polyhedra sharing successively an edge and a face (Figure 2a) and  $[\text{PS}_4]$  tetrahedra attached to the  $^{1-}[\text{Ce}_6\text{S}_6]$  skeleton through the sharing of three sulfur atoms ( $S(3)-S(4)-S(8)$  and  $S(1)-S(5)-S(6)$  for  $P(1)$  and  $P(2)$ , respectively) (Figure 2b). The structural arrangement of the  $^{1-}[\text{CeP}_2\text{S}_8]^{3-}$  chains recalls that of the  $^{1-}[\text{Nb}_2\text{PS}_{10}]$  chains in  $\text{KNb}_2\text{PS}_{10}$ <sup>19</sup> based on a  $^{1-}[\text{Nb}_2\text{S}_9]$  skeleton on which the  $[\text{PS}_4]$  tetrahedra are condensed. The bidimensional character of  $K_3CeP_2S_8$ , which is clearly observed from the morphology of the crystals, can be associated with the stacking, along the  $b$  axis, of  $^{2-}[\text{KCeP}_2\text{S}_8]^{2-}$  slabs and double alkali metal layers (Figure 1).

$K_3CeP_2S_8$  is a bright yellow material, and in order to shed light on the type of transition involved in the coloring process, self-

- (1) Sunshine, S. A.; Kang, D.; Ibers, J. A. *J. Am. Chem. Soc.* **1987**, *109*, 6202.
- (2) Kanatzidis, M. G.; Sutorik, A. C. *Prog. Inorg. Chem.* **1995**, *43*, 151 and references therein.
- (3) Kanatzidis, M. G. *Curr. Opin. Solid State Mater. Sci.* **1997**, *2*, 139 and references therein.
- (4) Wu, P.; Ibers, J. A. *J. Solid State Chem.* **1993**, *107*, 347.
- (5) Chen, J. H.; Dorhout, P. K. *Inorg. Chem.* **1995**, *34*, 5705.
- (6) Chen, J. H.; Dorhout, P. K.; Ostenson, J. E. *Inorg. Chem.* **1996**, *35*, 5627.
- (7) Christuk, A. E.; Wu, P.; Ibers, J. A. *J. Solid State Chem.* **1994**, *110*, 330.
- (8) Wu, P.; Christuck, A. E.; Ibers, J. A. *J. Solid State Chem.* **1994**, *110*, 337.
- (9) Bronger, W.; Müller, P. *J. Less-Comm. Met.* **1984**, *100*, 241.
- (10) Lu, Y.-J.; Ibers, J. A. *Comments Inorg. Chem.* **1993**, *14*, 229.
- (11) Elder, S. H.; Van der Lee, A.; Brec, A. *J. Solid State Chem.* **1995**, *116*, 107.
- (12) Sayettat, J. Ph.D. Thesis, University of Nantes, 1997.
- (13) Sayettat, J.; Jobic, S.; Gabriel, J.-C.; Bull, L.; Fourmigué, M.; Batail, P.; Brec, R.; Inglebert, E.-L.; Sourisseau, C. *J. Mater. Chem.*, submitted.
- (14)  $\text{KCeP}_2\text{S}_6$  crystallizes in the monoclinic space group  $P2_1/c$ , with  $a = 11.968(1)$  Å,  $b = 7.4728(4)$  Å,  $c = 11.3369(9)$  Å, and  $\beta = 109.567(8)^\circ$ , and  $\text{K}_2\text{CeP}_2\text{S}_7$  in the  $C2$  space group with  $a = 23.018(4)$  Å,  $b = 6.7776(9)$  Å,  $c = 8.994(2)$  Å, and  $\beta = 99.42(2)^\circ$ .
- (15) Gauthier, G.; Jobic, S.; Brec, R.; Rouxel, J. In preparation.

- (16) Crystals of  $K_3CeP_2S_8$  were prepared from a reaction of a mixture of  $\text{K}_2\text{S}$ ,  $\text{Ce}_2\text{S}_3$ ,  $\text{P}_2\text{S}_5$ , and  $\text{S}$  powders ( $\text{K}_2\text{S}$  (Cerac, 100 mesh, 99.9%), 174.4 mg, 1.0 mmol;  $\text{Ce}_2\text{S}_3$  (Cerac, 325 mesh, 99.9%) 188.2 mg, 0.5 mmol;  $\text{P}_2\text{S}_5$  (Merck, 99.8%) 61.9 mg, 2.0 mmol;  $\text{S}$  (Fluka, >99.999%) 96.2 mg, 3.0 mmol) that were ground together and loaded into a quartz tube. The tube was evacuated to  $10^{-3}$  Torr, sealed, and heated over a period of 75 h to 300 °C, maintained at 300 °C for 2 days, then heated at 800 °C over a period of 125 h, maintained at 800 °C for 7 days, and cooled to room temperature over 5 h. The sample was not single-phased and contained, with  $\text{K}_3\text{CeP}_2\text{S}_8$ , some amounts of  $\text{K}_2\text{CeP}_2\text{S}_7$  and  $\text{KCeP}_2\text{S}_6$ . A microprobe analysis was made on several platelike crystals by EDAX and yielded a  $\text{K}_3\text{Ce}_{1.2}\text{P}_{2.2}\text{S}_{8.3}$  composition. The crystals deteriorate in a few hours in air.

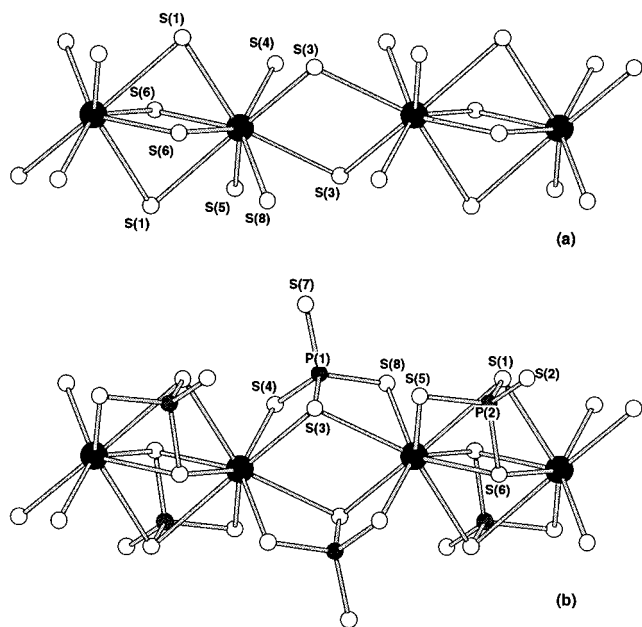


**Figure 2.** (a) Structural arrangement of 9-fold sulfur coordinated cerium polyhedra sharing edge and face, and defining the skeleton of the  $[\text{CeP}_2\text{S}_8]^{3-}$  chains. (b) View of a  $[\text{CeP}_2\text{S}_8]^{3-}$  chain fragment based on a  $[\text{CeS}_6]$  skeleton on which  $[\text{PS}_4]$  tetrahedra are condensed. Selected bond distances: Ce–S(1), 3.149(2) Å; Ce–S(1), 3.346(2) Å; Ce–S(3), 3.200(2) Å; Ce–S(3), 2.980(2) Å; Ce–S(4), 2.884(2) Å; Ce–S(5), 2.970(2) Å; Ce–S(6), 3.083(2) Å; Ce–S(6), 2.992(2) Å; Ce–S(8), 2.915(2) Å; Ce–P(1), 3.602(2) Å; Ce–P(1), 3.790(2) Å; Ce–P(2), 3.333(2) Å; Ce–P(2), 3.849(2) Å; P(1)–S(3), 2.070(3) Å; P(1)–S(4), 2.035(3) Å; P(1)–S(7), 2.005(3) Å; P(1)–S(8), 2.032(3) Å; P(2)–S(1), 2.050(3) Å; P(2)–S(2), 1.994(3) Å; P(2)–S(5), 2.024 Å; P(2)–S(6), 2.054(3) Å.

consistent ab initio structure calculations were performed using the TB-LMTO-ASA<sup>20–22</sup> method in its scalar relativistic version. As expected, the compound can be considered as a Zintl phase with a  $\text{K}_3\text{Ce}^{\text{III}}\text{P}^{\text{V}}_2\text{S}^{\text{II}}_8$  charge balance. Below  $-1.96$  eV (the zero energy being taken at the Fermi level) is located the valence band built upon S atomic orbitals. The Fermi level lies within the Ce-f block. A high density of states is calculated around  $E_f$  in relation

to a little band dispersion. This is in agreement with the small space extension of the f orbitals that do not allow them to hybridize substantially with the chalcogenide orbitals. On the other side of the Ce band, the conduction band lies above 0.69 eV: its bottom is constructed essentially upon Ce-d levels. From these electronic features, a semiconductor behavior is inferred. Under light excitation, and owing to the energy cost required to move an electron from one cerium to another ( $4f^1 + 4f^1 \rightarrow 4f^0 + 4f^2$ ) or from the valence band to the Ce- $4f^2$  level, it is more energetically favorable to promote an electron from the  $4f^1$  band to the conduction band. The yellow color of  $\text{K}_3\text{CeP}_2\text{S}_8$  results thus from the  $f \rightarrow d$  transition. The calculated gap (0.69 eV instead of the 2.5 eV expected value), although underestimated because of the difficulty of taking into account the localized f-orbital character in a band-like approach, is consistent with previous calculations for other types of colored cerium chalcogenides.<sup>23</sup> In red  $\gamma\text{-Ce}_2\text{S}_3$ , a similar transition mechanism has been proposed.<sup>24–26</sup> Hence, in going from  $\text{Ce}_2\text{S}_3$  to  $\text{K}_3\text{CeP}_2\text{S}_8$ , because of the yellow color observed for the latter, essentially an increase in the f-block  $\leftrightarrow$  conduction band gap energy is expected. With its strong covalent P–S bonds, it may be assumed that the presence of phosphorus implies an increase of the Ce–S chemical bond ionicity through an inductive effect. This means that in going from  $\text{Ce}_2\text{S}_3$  to  $\text{K}_3\text{CeP}_2\text{S}_8$ , a stabilization of the antibonding levels of the conduction band would take place with a decrease of the  $f \leftrightarrow d$  gap energy. However, this phenomenon would compete with a shift to lower energy of the occupied electronic f states through the decrease of the f electron screening effect from the cation nucleus due to the lessening of the covalent charge transfer. In view of the localized character of the f orbitals, this last effect must be preponderant, explaining the shifting of the absorption threshold from red to blue upon the insertion of phosphorus.

**Acknowledgment.** The research has been made possible by a grant (CIFRE 260/96) from Rhône-Poulenc Chimie and the “Association Nationale de la Recherche Technique”.

**Supporting Information Available:** Tables listing solution and refinement data, atomic positions, bond distances and angles, and anisotropic atomic displacement parameters (4 pages). Ordering information is given on any current masthead page.

IC980091P

- (17) Crystal structure data for  $\text{K}_3\text{CeP}_2\text{S}_8$ : monoclinic,  $a = 9.121(1)$  Å,  $b = 17.024(1)$  Å,  $c = 9.491(1)$  Å,  $\beta = 90.25(1)^\circ$ ,  $V = 1473.7$  Å<sup>3</sup>, space group  $P2_1/c$ ,  $Z = 4$ ,  $\rho_{\text{calc}} = 2.596$  g cm<sup>-3</sup>,  $\text{fw} = 575.84$  g mol<sup>-1</sup>,  $\mu(\text{Mo K}\alpha) = 52.5$  cm<sup>-1</sup>,  $2\theta_{\text{max}} = 56.3^\circ$ ,  $T = 291$  K, crystal size  $0.082 \times 0.015 \times 0.012$  mm<sup>3</sup>. The total data set consists of 12 555 reflections collected on a STOE Image Plate X-ray diffractometer. Images were recorded over a  $200^\circ$   $\phi$  range with a  $1^\circ$  increment angle and a 7 min irradiation per exposure; 3468 reflections were observed ( $I > 3\sigma(I)$ ); 1901 reflections were kept after averaging ( $R_{\text{int}} = 5.46\%$ ). The structure was determined from a Patterson map and successive Fourier and difference Fourier map analyses and followed by least-squares refinement on  $F$  with the JANA96<sup>18</sup> software package. No absorption correction was made. All atoms were refined anisotropically; 127 parameters were refined to  $R(F) = 0.030$ ,  $R_w(F) = 0.034$ ,  $\text{GOF} = 0.72$  based on a  $\sigma$  weighting scheme with an instability parameter of 0.03. The minimum and maximum residual electron density peaks in the difference map are  $-1.30$  and  $0.91$  e<sup>-</sup>/Å<sup>3</sup>.
- (18) Petøfèek, V.; Dusek, M. *JANA'98 Crystallographic Computing System*; Institute of Physics, Academy of Sciences of the Czech Republic: Praha, 1996.
- (19) Do, J.; Yung, H. *Inorg. Chem.* **1996**, *15*, 3729.

- (20) TB-LMTO-ASA: tight-binding linear muffin-tin orbital in the atomic sphere approximation. Program TB-LMTO, version 47, G. Krier, O. Jepsen, A. Burkhardt, and O. K. Andersen, Max-Planck-Institut für Festkörperforschung, D-70569 Stuttgart. All TB-LMTO-ASA calculations based on the LDA approximation were carried out by the use of the exchange correlation potential according to Barth and Hedin.<sup>21</sup> The radii of the muffin-tin spheres and necessary hollow spheres E within the framework of the ASA approximation are determined according to the method described by Jepsen and Andersen.<sup>22</sup>
- (21) Barth, U.; Ledin, L. *J. Phys. C* **1972**, *5*, 1629.
- (22) Jepsen, O.; Andersen, O. K. *Z. Phys. B* **1995**, *97*, 35.
- (23) Gauthier, G.; Kawasaki, S. J.; Brec, R.; Rouxel, J.; Macaudière, P. *J. Mater. Chem.* **1998**, *8*, 179.
- (24) Mauricot, R.; Gressier, P.; Evain, M.; Brec, R. *J. Alloys Compd.* **1995**, *223*, 130.
- (25) Perrin, M.-A.; Wimmer, E. *Phys. Rev. B* **1996**, *54*, 2428.
- (26) Zhukov, V.; Mauricot, R.; Gressier, P.; Evain, M. *J. Solid State Chem.* **1997**, *128*, 197.